

## MODELING SIMULTANEOUS HEAT AND MASS TRANSFER IN AN AMARANTH GRAIN DURING DRYING: A FINITE ELEMENT APPROACH

Ana M. Pagano<sup>a,c</sup> and Rodolfo H. Mascheroni<sup>b,c</sup>

<sup>a</sup> *Núcleo Tecnología de Semillas y Alimentos (TECSE), Área de Procesos, Depto. Ingeniería Química, Facultad de Ingeniería, Universidad Nacional del Centro de la Provincia de Buenos Aires, Av. Del Valle 5737, 7400 Olavarría, [apagano@fio.unicen.edu.ar](mailto:apagano@fio.unicen.edu.ar), <http://www.unicen.edu.ar>*

<sup>b</sup> *Centro de Investigación y Desarrollo en Criotecnología de Alimentos (CIDCA)-CONICET La Plata, Universidad Nacional de La Plata (UNLP)*

**Keywords:** drying simulation, thermal-mass analogy, amaranth, diffusion coefficient.

**Abstract.** A finite element formulation was used to obtain numerical solutions to the simultaneous equations of heat and mass diffusion that describe the removal of moisture and heat gain during the isothermal drying of amaranth grain, for temperatures from 25 to 70°C and initial moisture contents between 14.9 and 32.5% db (dry basis). The numerical model was implemented in ANSYS<sup>®</sup> using the direct analogy of thermal-mass diffusion. Granular particle was considered as homogeneous and isotropic material with negligible volume changes and constant properties evaluated at the initial moisture content. Grain shape was performed using different geometries (sphere, ellipsoid-oblate and volume of revolution). Given the symmetry of the grain, a two-dimensional model was defined taking into account only one quarter of the domain, which was discretized using 6-node triangular elements with characteristics of axial symmetry. As boundary condition, it was assumed that grain surface was instantaneously attained the equilibrium moisture content (i.e., strict internal control during the drying process). The effective coefficients of moisture ( $D_{ef}$ ) were estimated for each drying temperature and initial moisture content, and resulted between  $1.538 \times 10^{-12}$  m<sup>2</sup>/s and  $4.334 \times 10^{-11}$  m<sup>2</sup>/s when grain shape was modeled by an oblate ellipsoidal, and between  $1.850 \times 10^{-12}$  m<sup>2</sup>/s and  $5.189 \times 10^{-11}$  m<sup>2</sup>/s when a spherical geometry was considered, being the ratio between these coefficients ( $D_{ef \text{ ellipsoid}}/D_{ef \text{ sphere}}$ ) equivalent to the amaranth sphericity squared. The simulation results were validated by its contrast with their own experimental data of drying kinetics in thin layers. Best description of the drying curves was obtained when the domain was modeled by ellipsoidal geometry, followed by the spherical model. It was observed an Arrhenius type exponential dependence of the diffusion coefficient with the reciprocal of the absolute temperature, and a linear function of initial moisture content of grain. The activation energy for desorption of water was in the range 18.7–35.6 kJ/mol.

From the finite elements model it was possible to predict the profiles of moisture and temperature distribution inside the grain, allowing obtain the time process for reach the maximum thermal and mass gradients. Temperature profiles ensure the validity of the hypothesis assumed isothermal behavior of the solid during drying, because it was noted that the material quickly reaches equilibrium with the drying air temperature. The parameterized model developed has the flexibility to respond quickly to obtain the average moisture content of grain as a function of time and spatial distribution of moisture inside. Another strength of this simulation technique based on finite element method is that it allows to easily obtain moisture gradients (and, similarly, the thermal gradients) within the grain, in a form directly usable for any analysis stress cracking and can be extended the focus of this work to the study of other biomaterials with different geometries, loading conditions and boundary conditions.

## 1 INTRODUCTION

Amaranth is a plant native to America, domesticated, cultivated and used for over 4000 years, which has great importance in agriculture and food in the world due their exceptional particular characteristics. These include that the energy value of amaranth grain is greater than the cereals, having high protein content, somewhat greater in quantity and quality than that of other cereals (Weber, 1987; FAO, 1997).

The Organization of the United Nations Food and Agriculture Organization (FAO) and World Health Organization (WHO) confirmed that on an ideal protein value of 100, amaranth grain reaches 75, while soybean 68, wheat 60, and maize 44 (INTA, 2011).

Seeds and leaves are rich in proteins (16-18%) and have proper balance of essential amino acids, mainly lysine, methionine and tryptophan. Flours obtained from amaranth grain have multiple uses in human food as cookies, candy, tamales, tortillas, soft drinks and the leaves can be consumed as leafy vegetables with high economic and nutritional benefits. Other advantages are that have medicinal uses; inflorescences and leaves provide red pigments widely used in food coloring; is excellent in green matter production and use as a forage crop in livestock feed, including crop residues due the high protein content and appropriate digestibility.

The crop has easy adaptation to climatic conditions, soil and cropping systems. Is a C4 plant, efficient in water use, does not present photorespiration, has more efficient CO<sub>2</sub> fixation and produces the same amount of biomass with less water, with faster growth and greater ability to photo-assimilation than C3 plants under conditions of low rainfall. Unlike most food grains are grasses, dicot amaranth (widely adapted) offers new possibilities for crop rotation, introducing greater diversity in areas of monoculture, which can be useful for pest and disease control (FAO, 1997).

Argentina has potential areas for cultivation of Amaranth, mainly located in the Provinces of Jujuy, Santiago del Estero, Córdoba, East of La Pampa and Buenos Aires West (Abalone et al., 2004), where yields from 1800 to 2300 kg/ha –and exceptionally, 4500 kg/ha- have been reported (Tosi and Re, 2003; Abalone et al., 2004).

Amaranth grain must be harvested with a moisture content of about 30 % db (dry basis) or more to avoid great field losses; consequently, artificial drying is necessary to reduce the moisture level to about 10 % db (dry basis) to assure good preservation (Weber, 1987; Ronoh et al., 2010).

Postharvest handling of amaranth grain is critical for producing high-quality grain due to the smallness of seeds. Conventional drying systems are not adapted to the characteristics of this seed. Also, the use of silos for drying results limited due the high resistance to airflow that grains offer to the air passing through the depth of the grain bed (Abalone et al., 2004).

In order to develop appropriate technology of drying amaranth grain, thin-layer and bulk drying studies must be carried out. Many works has been reported in the literature concerning thin-layer drying of grains and other agriculture products, but very little information is available on amaranth (Tosi and Re, 1999; Lema et al., 2001; Vizcarra-Mendoza et al., 2003; Tironi et al., 2003; Calzetta Resio et al., 2004; Abalone et al., 2004; Pagano and Mascheroni, 2004, 2005, 2006).

The objective of present work is to evaluate the drying kinetics of amaranth grains under different conditions, and develop a simulation model to predict the grain moisture and temperature curves in time, analyzing the effect of the geometry assumed to approximate the grain shape on the effective diffusion coefficient of water, based in a finite elements approach.

As a precedent for other materials, [Muthukumarappan and Gunasekaran \(1990\)](#) who used the analytical solution of the mass transfer equation to predict the moisture absorption of corn grains considering different geometries: infinite slab, infinite cylinder and sphere, finding that the representation of the grain as an infinite slab was better to describe the experimental data ([Gastón et al., 2002](#)). [Gastón et al. \(2003\)](#) and [Gastón et al. \(2004\)](#) also evaluated the effect of using different geometries (spherical, ellipsoidal) to represent the grain of wheat on the diffusivity of water during drying.

[Wu et al. \(2004\)](#), seeking to achieve greater accuracy in describing the simultaneous transfer of heat and mass during the drying of rice, developed a theoretical model in three dimensions (3-D) characterizing the geometry of the grain using a system BFC ("body-fitted coordinates") and the finite volume method to solve partial differential equations, finding that the prediction of the maximum moisture gradient along the minor axis of the grain was comparable to that of a much more simple two-dimensional simulation model.

[Bakalis et al. \(2009\)](#) evaluated the water diffusivity in rice grains during cooking by the technique of finite element modeling the geometry of the grain as an axially symmetric ellipsoid. The authors considered the change in the volume of the grain as a result of water absorption during cooking and modeled the particle boundary domains using mobile and fixed boundary, showing identical performance for both models describe the experimental results.

In the present work, different geometries (sphere, ellipsoid of revolution and revolution volume) to approximate the shape and size of grain amaranth based on the same volume of the granular particle (pycnometric volume) were evaluated. For each of the geometries, external surface area and the corresponding volume were calculated, at each given initial moisture content, in order to define the  $a_v$  parameter in Becker's equation (Eqn. (5)).

To implement the simulation of the finite element model in ANSYS<sup>®</sup>, a transient thermal analysis (ANTYPE) was performed.

## 2 MATERIALS AND METHODS

### 2.1 Experimental data of drying of amaranth grain

Data of thin-layer drying of amaranth grain were obtained either from:

i) own experimental research ([Tironi et al., 2003](#); [Pagano and Mascheroni, 2006](#)) performed at temperatures between 20-55°C with constant airflow rate (0.3 m/s) and relative humidity, starting from 14.9% db (dry basis) of initial moisture content, and

ii) compiled data published in previous works ([Vizcarra-Mendoza et al., 2003](#); [Calzetta Resio et al., 2004](#); [Abalone et al., 2006a,b](#)) for other different conditions of initial moisture content (20-32% db), air temperatures (30-70°C) and velocities (0.3-3 m/s).

### 2.2 Mathematical modeling

There are four probable mechanisms to explain the water transfer during drying of solids ([Szöke et al., 1996](#); [Servieres and Giner, 1997](#)):

- i) movement of free water due to capillary forces;
- ii) liquid diffusion due to concentration gradients;
- iii) movement of water vapor due to pressure gradients;
- iv) diffusion in liquid layers absorbed in the solid interface.

However, in order to describe the loss of moisture during drying frequently is accepted that the phenomenon is controlled by the mechanism of liquid/vapor diffusion. For grains, during long time has been satisfactorily applied a simplification based on assuming that the heat

transfer effects can be negligible, then the drying process can be considered taking into account only the mass transfer. Consequently, this mechanism has been usually modeled by the solution of the microscopic balances in stationary state considering the Fick diffusion with constant coefficient and boundary conditions of first order.

To simulate what happens inside an amaranth grain during drying, water distribution in the grain can be determined by the model of [Steffe and Singh \(1979\)](#), based on the following assumptions:

- a) the mechanism of moisture movement is the spread of liquid;
- b) diffusion coefficients are not a function of concentration of moisture;
- e) the material component of amaranth grain is homogeneous and isotropic;
- f) volume reduction of amaranth grain during the drying process is negligible.

The differential equation that represents the process of moisture movement inside the kernel in equations in a Cartesian coordinate system ( $x, y, z$ ) can be expressed as ([Crank, 1964](#); [Holman, 1976](#); [Wu et al., 2004](#); [Madenci and Guven, 2006](#); [De Queiroz and Couto, 2006](#)):

$$\frac{\partial M}{\partial t} = D_{ef} \left( \frac{\partial^2 M}{\partial x^2} + \frac{\partial^2 M}{\partial y^2} + \frac{\partial^2 M}{\partial z^2} \right) \quad \text{in } \Omega \quad (1)$$

$$M(t=0) = M_o \quad \text{in } \Omega \quad (2)$$

$$M = M_e \quad \text{on } \Gamma \quad (3)$$

where  $M$  is the moisture content (% db);  $D_{ef}$  is the effective diffusion coefficient ( $\text{m}^2/\text{s}$ );  $t$  is the drying time (s);  $M_o$  and  $M_e$  are the initial and equilibrium moisture content (% db);  $\Omega$  represents the complete domain of the grain body; and  $\Gamma$  is their boundary surface.

The grain is assumed as a homogeneous and isotropic material, shrinkage during drying is considered negligible, and the mass diffusivity is assumed constant. The boundary condition pointed in Eqn. (3) involves that the equilibrium moisture content is attained instantaneously, so the process is strictly controlled by a diffusion mechanism ([Brooker et al., 1992](#); [Gastón et al., 2004](#)).

The analytic solution for the diffusion equation for spheres with radius  $r$  has the following expression ([Becker and Sallans, 1955](#); [Becker, 1959](#); [Giner and Mascheroni, 2002](#); [Márquez et al., 2006](#)):

$$MR = \frac{M - M_e}{M_o - M_e} = \frac{6}{\pi^2} \sum_{n=1}^{n=\infty} \frac{1}{n^2} \text{Exp} \left[ -n^2 \pi^2 \left( \frac{D_{ef} t}{R_p^2} \right) \right] \quad (4)$$

where  $MR$  is the normalized moisture ratio;  $R_p$  is the particle radius (m).

The infinite series of Eqn. (4) can be simplified to the first term of the series, but only for long times when  $MR < 0.3$ . For the practical range of foods drying ( $0.2 < MR < 1$ ), [Giner and Mascheroni \(2001\)](#) shown that a simplification to the analytical diffusion equation developed by [Becker \(1959\)](#), known as the “short-time” equation, can be applied to thin-layer drying of wheat without losing the accuracy of the standard infinite series solution for spheres. This equation for spherical geometry has the form:

$$MR = \frac{M - M_e}{M_o - M_e} = 1 - \frac{2}{\sqrt{\pi}} a_v \sqrt{D_{ef} t} + 0.331 a_v^2 D_{ef} t \quad (5)$$

where  $a_v$  is the surface area of particle per unit particle volume. In spheres,  $a_v=3/R_p$ .

### 2.3 Model of equilibrium moisture content

The equilibrium moisture content ( $M_e$ , % db) for each drying condition was estimated using the four-parameter GAB model developed in a previous work (Pagano and Mascheroni, 2004, 2005):

$$M_e = \frac{AC_o \text{Exp}(C_1/T_a) Ba_w}{(1 - Ba_w)(1 - Ba_w + BC_o \text{Exp}(C_1/T_a) a_w)} \quad (6)$$

where  $A$ ,  $B$ ,  $C_o$  and  $C_1$  are parameters for amaranth grain with values of 0.064; 0.731; 13.66 and 2.88, respectively.

### 2.4 Equations for thermal properties

In order to obtain the profiles of temperature during drying, the following properties were used for solving the thermal problem:

The density of grain amaranth ( $\rho$ ) was evaluated based on the densities of its components: 65.1% carbohydrates; 12.9% proteins; 7.2% lipids; 6.7% fibers; 2.5% ash; 12.3% water (FAO, 1999) through the following expression (Choi and Okos (1986) in Ibarz-Ribas and Barbosa-Cánovas, 2005):

$$\rho = \frac{1}{\sum_i \left( \frac{x_i^m}{\rho_i} \right)} \quad (7)$$

where  $x_i^m$  is the mass fraction of the component  $i$ ; and  $\rho_i$  is the density of that component.

The densities of the amaranth grain components were estimated by the corresponding correlations shown in Table 1, at each experimental temperature.

The thermal conductivity  $k$  was estimated using the next equation (Ibarz-Ribas and Barbosa-Cánovas, 2005):

$$k = \sum_i (k_i X_i^V) \quad (8)$$

where  $k_i$  is the thermal conductivity of component  $i$ ; and  $X_i^V$  is the volume fraction of that component. The volume fraction of component is given by:

$$X_i^V = \frac{x_i^m / \rho_i}{\sum_i \left( \frac{x_i^m}{\rho_i} \right)} \quad (9)$$

The thermal conductivity of each of the components of the grain was estimated from the equations presented in Table 1; these equations were proposed by Choi and Okos (1986) (in Ibarz-Ribas and Barbosa-Cánovas, 2005) to calculate  $k$  for each component of the material, depending on the drying temperature of each experimental condition.

| Component     | Property                                   | Equation  |
|---------------|--|---|
| Carbohydrates | Density,<br>$\rho$<br>(kg/m <sup>3</sup> ) | $1599.1 - 0.31046 T$  |
| Ash           |  | $2423.8 - 0.28063 T$  |
| Fibers        |  | $1311.5 - 0.36589 T$  |
| Lipids        |  | $925.59 - 0.41757 T$  |
| Proteins      |  | $1329.9 - 0.5184 T$   |
| Water         |  | $997.18 + 0.0031439 T - 0.0037574 T^2$                          |
| Carbohydrates | Thermal<br>conductivity,<br>$k$<br>(W/m K) | $0.20141 + 1.3874 \times 10^{-3} T - 4.3312 \times 10^{-6} T^2$ |
| Ash           |  | $0.32962 + 1.4011 \times 10^{-3} T - 2.9069 \times 10^{-6} T^2$ |
| Fibers        |  | $0.18331 + 1.2497 \times 10^{-3} T - 3.1683 \times 10^{-6} T^2$ |
| Lipids        |  | $0.18071 + 2.7604 \times 10^{-3} T - 1.7749 \times 10^{-6} T^2$ |
| Proteins      |  | $0.17881 + 1.1958 \times 10^{-3} T - 2.7178 \times 10^{-6} T^2$ |
| Water         |  | $0.57109 + 1.7625 \times 10^{-3} T - 6.7036 \times 10^{-6} T^2$ |
| Carbohydrates | Specific heat,<br>$C_p$<br>(kJ/kg K)       | $1.5488 + 1.9625 \times 10^{-3} T - 5.9399 \times 10^{-6} T^2$  |
| Ash           |  | $1.8459 + 1.8306 \times 10^{-3} T - 4.6509 \times 10^{-6} T^2$  |
| Fibers        |  | $1.0926 + 1.8896 \times 10^{-3} T - 3.6817 \times 10^{-6} T^2$  |
| Lipids        |  | $1.9842 + 1.4733 \times 10^{-3} T - 4.8008 \times 10^{-6} T^2$  |
| Proteins      |  | $2.0082 + 1.2089 \times 10^{-3} T - 1.3129 \times 10^{-6} T^2$  |
| Water         |  | $4.1762 - 9.0864 \times 10^{-5} T + 5.4731 \times 10^{-6} T^2$  |

Table 1: Equations for calculating properties of food components (Ibarz-Ribas and Barbosa-Cánovas, 2005).

Just as the density, the specific heat of grain ( $C_p$ ) was assessed for each experimental condition of temperature using the equations listed in Table 1 (Ibarz-Ribas and Barbosa-Cánovas, 2005).

The coefficient of heat transfer by convection  $h_c$  (W/m<sup>2</sup> K) was evaluated from the following equation for each experimental condition (Wu et al., 2004):

$$h_c = 16.09 + 65.87 V^{0.53} \quad (10)$$

where  $V$  is the velocity of the drying air (m/s).

## 2.5 Geometry for grain shape dimensional description

To resolve the microscopic steady-state balance considering Fick diffusion with constant coefficient and boundary conditions of first order, previously it is necessary to define the proper geometry to describe the shape and dimensions of the granular particle, then apply the corresponding analytical solution considering the assumed geometry.

To represent the shape of grain amaranth, different models of geometric approaches were considered, a sphere, an oblate ellipsoid with two characteristic diameters (spheroid), and a volume of revolution formed by the union between two concentric oblate ellipsoids, each of them with two characteristic diameters (Figs. 1a-c). In all cases, the volumes of the bodies were defined as a volume equivalent to the own grain volume (pycnometric volume  $V_g$ ). This pycnometric volume was evaluated at each initial grain moisture content ( $M_o$ : 14.9% db; 20% db; 32.5% db) using the following correlation (Abalone et al., 2004).

$$V_g = (0.493 + 0.00611 M_o) 10^{-9} \quad (11)$$

The equivalent diameter ( $D_{eq}$ ) for the equivalent sphere, the diameters equatorial ( $e_1$ ) and polar ( $e_2$ ) for the equivalent oblate ellipsoid, and the two equatorial diameters ( $e_1$ ,  $e_5$ ) and polar diameters ( $e_4$ ,  $e_6$ ) for the equivalent volume of revolution were considered constant during grain drying.

To get the volume of the oblate ellipsoid or spheroid ( $e_1 > e_2$ ) coincident with the actual

volume of the grain, it was assumed that the semi-major axis of the ellipsoid ( $e_1$ ) is equal to half of the average characteristic length calculated between the length and the width of the grain; while the semi-minor axis ( $e_2$ ) was calculated in order to meet the proposed target ( $V_{elipsoide} = (4\pi/3) e_2 e_1^2 = V_g$ ). This procedure was proposed by [Abalone et al. \(2004\)](#).

The equivalent diameter of a sphere with the same volume as the grain ( $D_{eq}$ ) and the geometric parameters corresponding to the semi major axis ( $e_1$ ) and eccentricity ( $\xi$ ) of the ellipsoid at each initial moisture content were estimated on the basis of the following correlations ([Abalone et al., 2004](#)).

$$D_{eq} = (0.987 + 0.00341 M_o) 10^{-3} \quad (12)$$

$$e_1 = (0.625 + 0.00203 M_o) 10^{-3} \quad (13)$$

$$\xi = \sqrt{1 - (e_2/e_1)^2} \quad (14)$$

The semi-minor axis ( $e_2$ ) of the spheroid was calculated from  $V_g$  and  $e_1$ , and was expressed in terms of initial moisture content according to the equation ([Abalone et al., 2004](#)):

$$e_2 = (0.308 + 0.00119 M_o) 10^{-3} \quad (15)$$

In the same direction, the semi-axis of the two ellipsoids that conformed the volume of revolution ( $e_3, e_4, e_5, e_6$ ) were calculated by the following equations reported by [Abalone et al. \(2004\)](#), being  $e_3$  equal to half mean value between the length and the width of the grain, while  $e_6$  was the half of the grain thickness.

$$e_3 = (0.625 + 0.00203 M_o) 10^{-3} \quad (16)$$

$$e_4 = (0.231 + 0.00098 M_o) 10^{-3} \quad (17)$$

$$e_5 = (0.481 + 0.00157 M_o) 10^{-3} \quad (18)$$

$$e_6 = (0.393 + 0.00168 M_o) 10^{-3} \quad (19)$$

Another geometric parameter, the sphericity (or shape factor,  $\phi$ ), that defines the approximation of the grain shape to a sphere, was evaluated as the rate between the surface of a sphere with the same volume of the grain, and the surface of the particle described by a regular geometry ([Becker, 1959](#); [Aguerre et al., 1987](#); [Álvarez et al., 1995](#)), being the following expression for ellipsoid:

$$\phi = \frac{\pi D_{eq}^2}{2\pi e_1^2 + \pi \frac{e_2^2}{\xi} \ln\left[\frac{(1+\xi)}{(1-\xi)}\right]} \quad (20)$$

The external surface ( $S$ ) and the volume ( $V$ ) of the spherical and ellipsoidal particles were calculated from the geometric parameters  $D_{eq}$ ,  $e_1$  and  $e_2$ , in order to estimate the specific area ( $a_v = S/V$ ) included into the “short times” model of (Eqn. (5)). After this, the following expressions were devised to relate the specific area with the initial moisture content.

$$a_{v \text{ sphere}} = \frac{S_{\text{sphere}}}{V_{\text{sphere}}} = 6047.6 - 17.939 M_o \quad (R^2=0.9998) \quad (21)$$

$$a_{v \text{ ellipsoid}} = \frac{S_{\text{ellipsoid}}}{V_{\text{ellipsoid}}} = 6645 - 20.491 M_o \quad (R^2=0.9998) \quad (22)$$

Analogous expression has been reported by [Giner and Mascheroni \(2002\)](#) to describe the relationship between the specific surface area and the initial moisture content for wheat.

For the volume of revolution, the specific area was calculated from the following expression based on correlations of  $S_{\text{vol.revol.}}$  and  $V_{\text{vol.revol.}}$  with  $M_o$  planned starting from reported data by [Abalone et al. \(2004\)](#):

$$a_{v \text{ vol revol}} = \frac{S_{\text{vol.revol.}}}{V_{\text{vol.revol.}}} = \frac{2.56 \times 10^{-8} M_o + 3.3475 \times 10^{-6}}{6.1 \times 10^{-12} M_o + 4.927 \times 10^{-10}} \quad (R^2=0.9995) \quad (23)$$

## 2.6 Analogy between the processes of mass transfer and heat transfer

Equation (1) is analogous to the heat diffusion equation in non-stationary state that can be expressed as ([Madenci and Guven, 2006](#)):

$$\frac{\partial T}{\partial t} = \frac{k}{\rho_g c_g} \left( \frac{\partial^2 T}{\partial x^2} + \frac{\partial^2 T}{\partial y^2} + \frac{\partial^2 T}{\partial z^2} \right) \quad (24)$$

with boundary and initial conditions of  $-k \partial T / \partial n = h_c (T - T_e)$  when  $T(t=0) = T_o$ , where  $k$  is the thermal conductivity (W/m °C);  $\rho_g$  is the kernel density (kg/m<sup>3</sup>);  $c_g$  is the grain specific heat capacity (J/kg °C);  $T$  is the temperature (K);  $n$  is the gradient normal to kernel surface;  $h_c$  is convective heat transfer coefficient (W/m<sup>2</sup> K);  $T_e$  is the temperature of the environment surrounding the kernel (°C); and  $T_o$  is the initial temperature of the kernel (°C).

Although Eqns. (1) and (24) are analogous, the formulation of finite elements for heat transfer cannot be directly applied for the resolution of the moisture diffusion problems for multiple dissimilar materials, due the moisture concentration is not continuous across the material interfaces, unlike occurs with the temperature ([Madenci and Guven, 2006](#)).

However, when moisture concentration is normalized with respect to the equilibrium moisture content ( $C_e$ ) for water desorption, or with respect to the saturated moisture content ( $C_{sat}$ ) for the water absorption, this incompatibility disappears and the formulation for heat diffusion can be applied to solve mass transfer problems (like drying and humectation). The normalized moisture, called wetness ( $w$ ) or moisture parameter is written as  $w = C/C_{sat}$  or  $C/C_e$  ([Madenci and Guven, 2006](#)).

[Yoon and Han \(2007\)](#) analyzed the domains where this methodology for resolution of mass transfer problems based on the resolution of the thermal problem can be applied. They evaluated two different schemes: the direct thermal-mass analogy and the normalized thermal-mass analogy, concluding that the direct analogy is valid for single materials and the normalized analogy can be extended for multiple materials if the thermal loads are spatially and temporally isothermal.

## 2.7 Modeling based on finite elements approach

It is clear that for solving a heat diffusion problem by Eqn. (24), the properties of thermal conductivity  $k$ , specific heat  $c$ , and density  $\rho$  must be known. In the formulation of moisture diffusion problem for resolution by analogy with heat diffusion problem, one possibility is to use the parameter  $w$ . In that case, the following correspondence presented in [Table 1](#) must be considered during the data load of the material in ANSYS<sup>®</sup>. Then, once the solution is

obtained, the weight of water lost in an element  $W^{(e)}$  is determined by the product between the average concentration and the volume element  $V^{(e)}$  as follows; the total weight of moisture lost by the material can be calculated directly by summing the weights of water lost in each of the elements.

$$W^{(e)} = \left( \frac{1}{N} \sum_{i=1}^N w_i C_{sat} \right) V^{(e)} \quad (25)$$

where  $N$  is the number of elements;  $V^{(e)}$  is the element volume;  $w_i$  is the parameter of moisture in the  $i^{th}$  node.

| Property             | Heat transfer               | Mass transfer  |
|----------------------|-----------------------------|--|
| Primary variable     | temperature, $T$            | wetness, $w$   |
| Density              | $\rho$ (kg/m <sup>3</sup> ) | 1  |
| Thermal conductivity | $k$ (W/m °C)                | $D * C_{sat}$ (absorption)<br>$D * C_e$ (desorption) |
| Specific heat        | $c$ (J/kg °C)               | $C_{sat}$ (absorption)<br>$C_e$ (desorption)         |

Table 1: Correspondence for the thermal diffusion- mass diffusion analogy

Another possibility for solving the problem of moisture diffusion by analogy with the problem of thermal diffusion is to consider simultaneously the density and specific heat equal to one (De Queiroz and Couto, 2006). This last approach was applied in the present work.

Assuming negligible change of density, the mean grain moisture content can be calculated at any time using the nodal values following the procedure described by Haghghi and Segerlind (1988) (Gastón y colab., 2002; Abalone y colab., 2000).

### Sphere

In first place, in virtue of the symmetry of the problem for spherical geometry, a two-dimensional domain considering only an octave part of the projected area of the sphere was taken into account. For the construction of the model of finite elements, the domain was discretized using bi-dimensional triangular elements of six nodes (PLANE77) with characteristics of axial symmetry.

The model was parametrically defined through the specification of the following parameters:

- Initial moisture content of grain ( $M_o$ )
- Equivalent diameter of grain ( $D_{eq}$ )
- Equilibrium moisture content of grain ( $M_e$ )
- Effective diffusion coefficient of moisture in grain ( $D_{ef}$ ) for spherical geometry
- Total time of drying ( $TIME$ )
- Time increment for the drying simulation ( $INCR$ )

The initial moisture content parameter was fixed at each initial moisture content of the whole of experimental data (14.9; 20; 32.5% db); for the equivalent diameter ( $D_{eq}$ ) was assigned values calculated by Eqn. (12) at each initial moisture content, while for the equilibrium moisture content was selected the values estimated by Eqn. (6) at each

experimental condition of drying temperature and relative humidity.

For the parameter of moisture diffusion coefficient  $D_{ef}$ , the values resulting from the model of “short-times” for spheres (Eqn. (5)) fitted to the experimental data were used as input.

The parameter  $TIME$  were defined as the final drying time of each drying curve, and the parameter  $INCR$  was calculated like  $TIME/30$  in order to obtain 30 sub-step in the drying simulation.

The material properties specific density and specific heat were defined as unitary values, while the thermal conductivity was fixed by analogy like the moisture diffusion coefficient at each condition (De Queiroz and Couto, 2006).

The domain was modeled using primitive entities in Cartesian coordinates. Structured automatic meshing based on 6-nodes triangular elements (Figure 1a) was used, taking into account that the internal angles of the elements were lesser than  $90^\circ$  in order to avoid numerical oscillations (Haghighi and Segerlind, 1988).

### Ellipsoid

The grain shape was considered as an oblate ellipsoid (spheroid). Due the symmetry of the problem, a two-dimensional domain considering only a quarter of the projected area by a spheroid with the same volume that the grain was assumed. The model was parametrically defined through the specification of the semi-axis of the oblate ( $e_1$ ,  $e_2$ ) which were calculated by Eqns. (13) and (15). As was proceeded with spherical geometry, also  $M_o$ ,  $M_e$ ,  $D_{ef}$  for ellipsoidal geometry,  $TIME$  and  $INCR$  were defined as parameters. The domain was also discretized using 6-nodes triangular elements (PLANE77) with axial symmetry (Figure 1b).

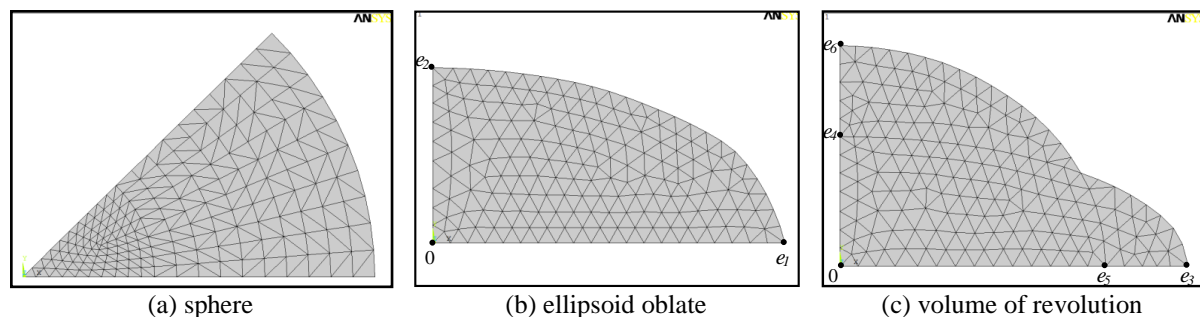


Figure 1: Discretization of the two-dimensional domain considered to represent the grain amaranth by a spherical geometry in the analysis of drying by the finite element method.

### Volume of revolution

The grain shape was represented by the union of two oblate ellipsoids with the same volume that the grain; only a quarter of the projected area by this volume of revolution was assumed as domain. The semi-axis of both spheroids ( $e_3$ ,  $e_4$ ,  $e_5$ ,  $e_6$ ) were calculated by Eqns. (16) a (19) as parameters of the model of simulation. Likewise that for the sphere, values of  $M_o$ ,  $M_e$ ,  $D_{ef}$  (for geometry of volume of revolution),  $TIME$  and  $INCR$  were defined as parameters. Also, the domain was discretized by 6-node triangular elements axially symmetrical (Figure 1c).

### Definition of the material properties

When taken unitary the specific gravity and the specific heat for solving the diffusion problem by analogy with the thermal problem, the only necessary material property required

by the ANSYS element type PLANE77 is the diffusivity of moisture, as noted above (De Queiroz and Couto, 2006). Then, each of the geometrical models developed to represent the grain shape was simulated using as input parameter values of the diffusivity of water (representing the thermal conductivity of the material by analogy) obtained from statistical fitting of the mathematical equation of "short time" to experimental data, as will be shown later.

### ***Application of loads on the finite elements model***

For all geometries considered and for each experimental condition simulated drying, thermal loads were applied on the model considering uniform temperature (*TUNIF*) throughout the domain as initial condition (which was admitted by analogy as the moisture content  $M_o$  initial for each case). As boundary condition, constant temperature (*TEMP*) at the nodes of grain surface was entered (by analogy, the equilibrium moisture content  $M_e$  for each of the experimental condition).

### ***Definition of the controls for resolution / solution***

For time, frequency and time increment for each sub-step, adequate controls were defined according to each one of the drying curves, to avoid numerical oscillations, and the results of each sub-step were stored in a file.

### ***Post-processing of results***

Once the solution was obtained, the results of the nodal temperatures at each time (sub-step) representing the moisture content at each node, were read in the post-processing stage (POST1). From these data it was possible to determine and the spatial distribution of grain moisture content (Contour Nodal Solution Data) for each time interval.

Also, animations were performed to observe, spatially and temporally, the variation of the moisture content through the representation of the nodal temperatures (analogous to the nodal moisture content).

## **3 RESULTS AND DISCUSSION**

### **3.1 Mathematical fitting of the drying curves**

The effective coefficients of moisture ( $D_{ef}$ ) were estimated by fitting Eqn. (5) to the experimental data for each drying temperature and initial moisture content. The results shown in Table 2, shows the good agreement of the mathematical equation of "short time" with the drying curves observed: correlation coefficients ( $R^2$ ) above 0.982 ( $0.982 \leq R^2 \leq 0.998$ ), and low mean relative deviations ( $p$ ) lesser than 10% ( $0.028 \leq p \leq 0.115$ ) in most cases were obtained.

When grain shape was modeled by an oblate ellipsoidal, the effective diffusion coefficients resulted between  $1.538 \times 10^{-12}$  m<sup>2</sup>/s and  $4.334 \times 10^{-11}$  m<sup>2</sup>/s, and when a spherical geometry was considered, the coefficients were between  $1.850 \times 10^{-12}$  m<sup>2</sup>/s and  $5.189 \times 10^{-11}$  m<sup>2</sup>/s.

The ratio between these coefficients was equivalent to the amaranth sphericity squared ( $D_{ef\ ellipsoid} / D_{ef\ sphere} = \phi^2$ ;  $R^2=0.98$ ), in concordance with the behavior reported by Aguerre et al. (1987) for corn, and also by others researchers (Gabbito and Aguerre, 1986; Gastón et al., 2002; Gastón et al., 2004; Waezi-Zadeh et al., 2010; Ruiz-López et al., 2011). This expression allows avoiding the geometry aberration error in amaranth diffusion coefficients in spherical geometries that round in average of about 17%. Gastón et al. (2004), analyzing the coefficient

of moisture diffusion in wheat, recommended this ratio  $D_{ef\ ellipsoid} / D_{ef\ sphere} = \phi^2$  to estimate diffusion coefficients of complex geometries starting from the correction of the diffusion coefficient of spheres and vice versa.

| $T$ (°C) | $M_o$ (% db) | $D_{ef\ sphere}$ (m <sup>2</sup> /s) | $D_{ef\ ellipsoid}$ (m <sup>2</sup> /s) | $D_{ef\ vol.revol.}$ (m <sup>2</sup> /s) |
|----------|--------------|--------------------------------------|---|--|
| 40       | 20           | $6.375 \times 10^{-12}$              | $5.303 \times 10^{-12}$                 | $5.228 \times 10^{-12}$                  |
| 50       |              | $8.719 \times 10^{-12}$              | $7.253 \times 10^{-12}$                 | $7.150 \times 10^{-12}$                  |
| 60       |              | $1.013 \times 10^{-11}$              | $8.424 \times 10^{-12}$                 | $8.308 \times 10^{-12}$                  |
| 70       |              | $1.218 \times 10^{-11}$              | $1.014 \times 10^{-11}$                 | $9.986 \times 10^{-12}$                  |
| 40       | 32.5         | $1.619 \times 10^{-11}$              | $1.352 \times 10^{-11}$                 | $2.060 \times 10^{-11}$                  |
| 50       |              | $2.496 \times 10^{-11}$              | $2.084 \times 10^{-11}$                 | $3.176 \times 10^{-11}$                  |
| 60       |              | $4.021 \times 10^{-11}$              | $3.357 \times 10^{-11}$                 | $5.116 \times 10^{-11}$                  |
| 70       |              | $5.189 \times 10^{-11}$              | $4.334 \times 10^{-11}$                 | $6.603 \times 10^{-11}$                  |
| 25       | 14.9         | $2.103 \times 10^{-12}$              | $1.748 \times 10^{-12}$                 | $1.742 \times 10^{-12}$                  |
| 30       |              | $1.850 \times 10^{-12}$              | $1.538 \times 10^{-12}$                 | $1.533 \times 10^{-12}$                  |
| 35       |              | $2.315 \times 10^{-12}$              | $1.924 \times 10^{-12}$                 | $1.918 \times 10^{-12}$                  |
| 40       |              | $2.255 \times 10^{-12}$              | $1.875 \times 10^{-12}$                 | $1.868 \times 10^{-12}$                  |
| 45       |              | $3.312 \times 10^{-12}$              | $2.753 \times 10^{-12}$                 | $2.744 \times 10^{-12}$                  |
| 50       |              | $4.079 \times 10^{-12}$              | $3.390 \times 10^{-12}$                 | $3.379 \times 10^{-12}$                  |
| 55       |              | $3.966 \times 10^{-12}$              | $3.295 \times 10^{-12}$                 | $3.285 \times 10^{-12}$                  |

Table 2: Coefficients of moisture diffusion for amaranth grains modeled by different geometries.

This relationship between the diffusion coefficients of ellipsoid and sphere is the reciprocal of the existing relationship between the specific areas of these geometric bodies:  $a_{v\ sphere} / a_{v\ ellipsoid} = \phi^2$ ; then, can be used i.e. the rate of specific areas  $a_{v\ sphere} / a_{v\ vol.revol.}$  to correct the diffusion coefficient of the sphere in order to obtain the diffusion coefficient of the volume of revolution (fifth column in Table 2).

Analyzing the relationship between the diffusion coefficients and the drying conditions (temperature and initial moisture content of grain), in a first step, it was observed an Arrhenius type exponential dependence of the diffusion coefficient with the reciprocal of the absolute temperature:

$$\ln(D_{ef}) = \ln(D_o) - \frac{E_a}{R_g T_a} \quad (26)$$

where  $D_o$  is the pre-exponential factor (m<sup>2</sup>/s);  $E_a$  is the activation energy (kJ/mol);  $R_g$  is 8.314 J/mol K; and  $T_a$  is the absolute temperature of drying (K).

From analysis of nonlinear regression, the activation energy for desorption of water was determined in the range 18.7–35.6 kJ/mol ( $R^2 > 0.999$ ).

Additionally, statistically was probed the influence of the initial moisture content of grain on the diffusion coefficient, proposing a linear function for describe the relationship between  $D_{ef}$  and  $M_o$ , which was incorporated into the pre-exponential factor.

$$D_{ef} = \left( D_{o1} + D_{o2} \left( \frac{M_o}{100} - 0.149 \right) \right) \exp \left( \frac{-\bar{E}_a}{R_g T_a} \right) \quad (27)$$

where  $D_{o1}$  and  $D_{o2}$  are constants ( $\text{m}^2/\text{s}$ ) with values of  $2.151 \times 10^{-8}$  and  $1.791 \times 10^{-6}$  for spheres ( $R^2 > 0.984$ ), while  $1.771 \times 10^{-8}$  and  $1.723 \times 10^{-6}$  for ellipsoids ( $R^2 > 0.984$ ); being  $\bar{E}_a$  the mean activation energy (25.1 kJ/mol).

Similar correlations between the diffusion coefficient, the temperature, and the initial moisture content have been reported by numerous researchers for different foods (Lu and Siebenmorgen, 1992; López et al., 1995; Madamba et al., 1996; Giner and Mascheroni, 2001, 2002; Panchariya et al., 2002; Vizcarra-Mendoza et al., 2003; Doymaz and Pala, 2003; Demirel and Turhan, 2003; Gastón et al., 2004; Mohapatra and Rao, 2005; Doymaz, 2005).

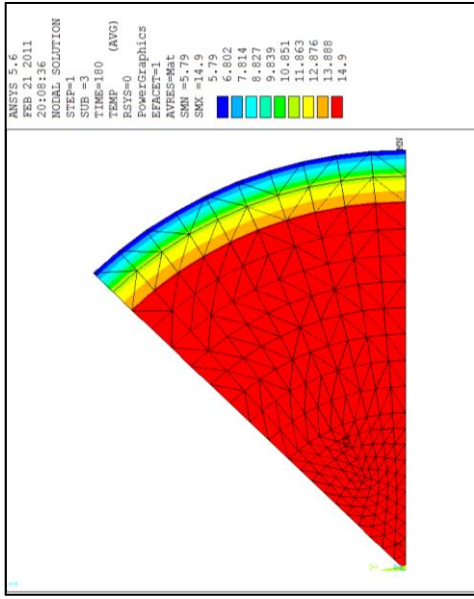
### 3.2 Simulation of the drying curves by models of finite elements

The values of the effective diffusion coefficients were used as input data (material property) for the finite element model. Different combinations of geometries to describe the amaranth grain (sphere, ellipsoid, volume of revolution) and diffusion coefficients ( $D_{ef \text{ sphere}}$ ,  $D_{ef \text{ ellipsoid}}$ ,  $D_{ef \text{ vol.revolution}}$ ) were used in order to evaluate the better performance of the finite elements model to reproduce the experimental drying data. The following Figure 2 to Figure 7 show the profiles of nodal moisture (by analogy of nodal temperature) at several time during the drying process.

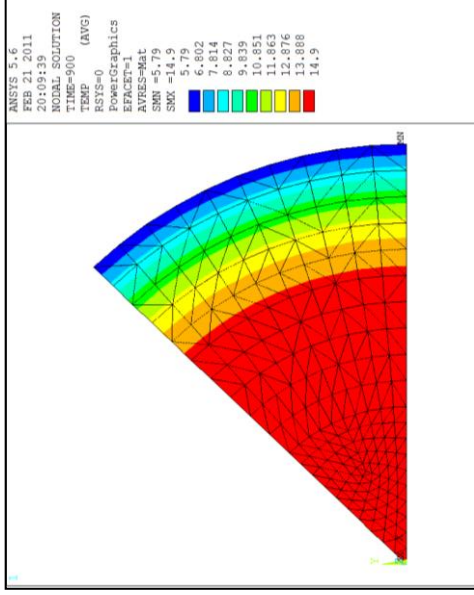
The profiles of moisture represent the evolution of the drying process in time and space. At fixed time, it can be noted that the profiles of the different geometries are dissimilar, giving different distributions of average moisture. On the other hand, for a given geometry, the moisture profiles at a fixed time instant are also different when different diffusion coefficients obtained for a particular geometry are applied: i.e., for ellipsoidal geometry, Figure 3c and Figure 4c evidence that the moisture distributions differ one of the other when diffusion coefficients obtained for spheres or ellipsoids are used.

So as to select the best combination geometry/diffusion coefficient, the simulation results were validated by its contrast with the experimental data of drying kinetics in thin layers. Best description of the drying curves was obtained when the domain was modeled by ellipsoidal geometry, followed by the spherical model. As example at two singular experimental conditions, Figure 8 and Figure 9 illustrate the drying curves predicted by the simulation of the finite elements models developed for different geometric shapes using different diffusion coefficients. Analogous behaviors were obtained for the other process conditions.

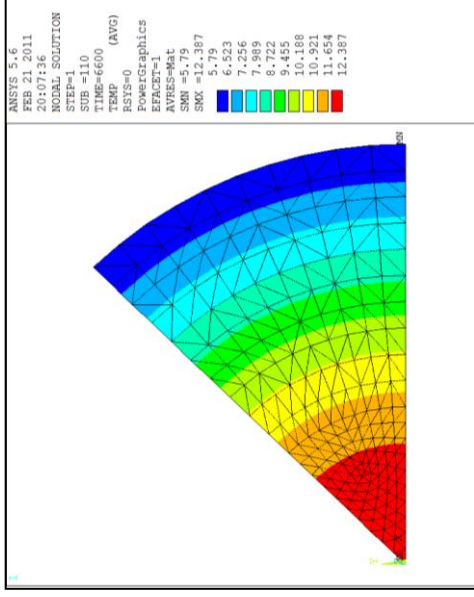
When spherical geometry was used to represent the grain shape, in general lesser drying rates were obtained. As can be seen in Figure 8 and Figure 9, the ellipsoids higher drying rates predicted regardless of the diffusion coefficient has been used,  $D_{ef \text{ ellipsoid}}$  or  $D_{ef \text{ sphere}}$ . This result is fully coincident with the behavior reported by Gastón et al. (2001a, 2001b, 2002) for wheat. These researchers demonstrated that when the mass diffusivity estimated with spherical geometry is used to predict drying curves of wheat assuming the grain shape as an axisymmetric ellipsoid, the predicted drying rate results higher than the experimental one (Gastón et al., 2003). This effect is explained by the fact that, being the volume for both geometries equal to the grain volume, the surface area for mass transfer is greater for ellipsoids than it is in the spheres.



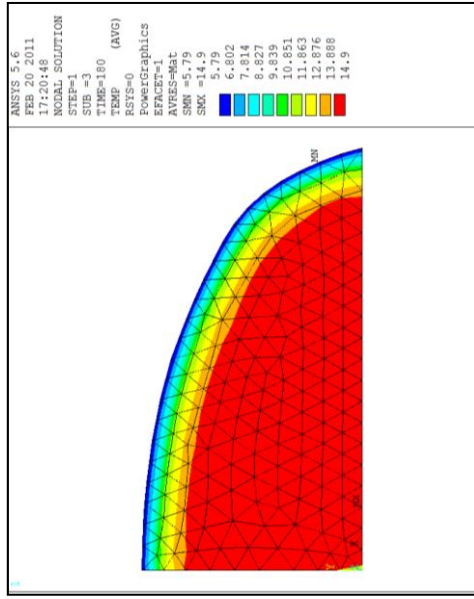
a)  $t = 180$  s



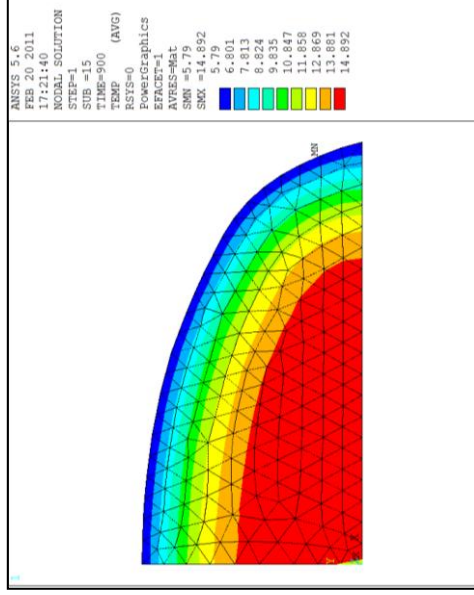
b)  $t = 900$  s



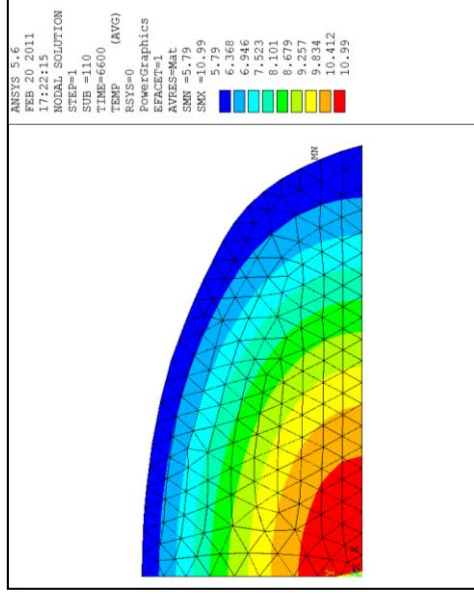
c)  $t = 6600$  s



a)  $t = 180$  s



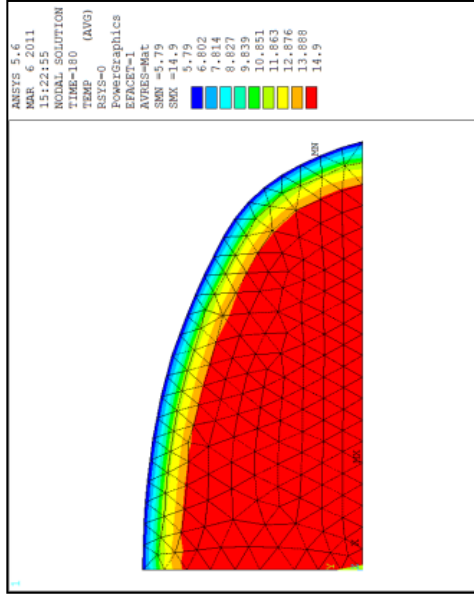
b)  $t = 900$  s



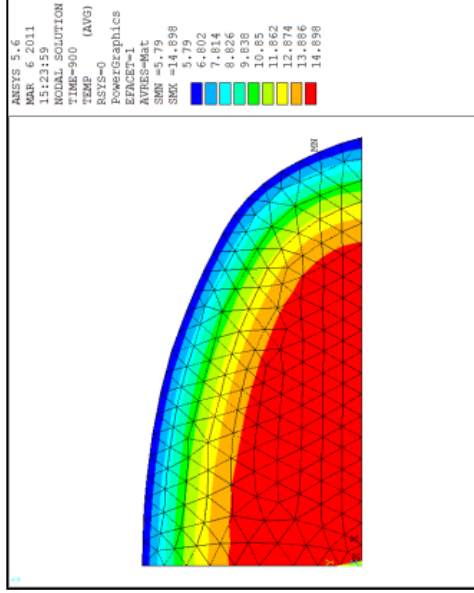
c)  $t = 6600$  s

Figure 2: Using “spherical” mass-diffusivity of to predict moisture profiles in the sphere.

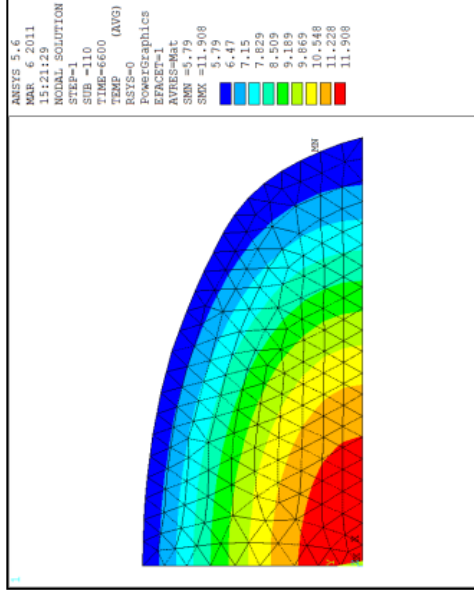
Figure 3: Using “spherical” mass-diffusivity of to predict moisture profiles in the ellipsoid oblate.



a)  $t = 180$  s

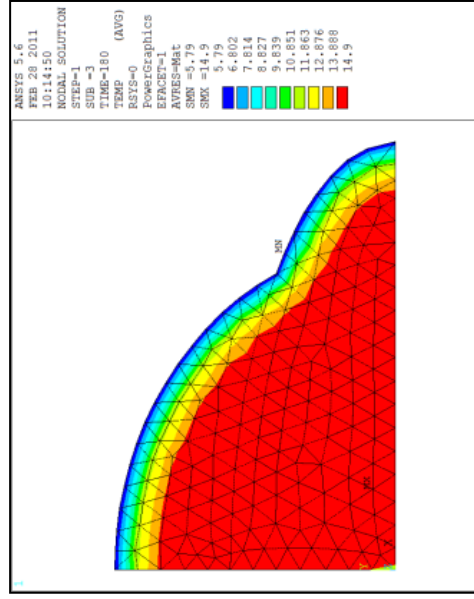


b)  $t = 900$  s

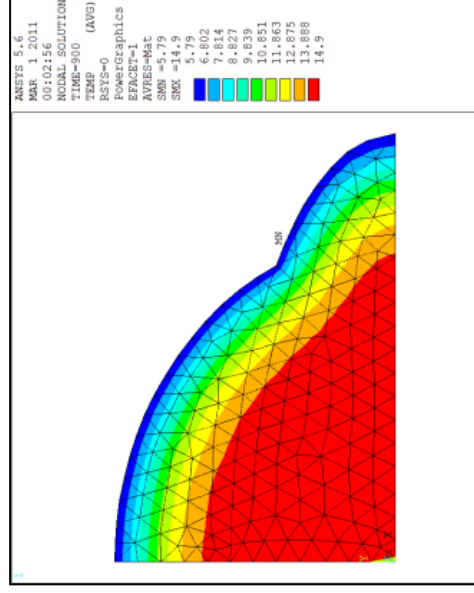


c)  $t = 6600$  s

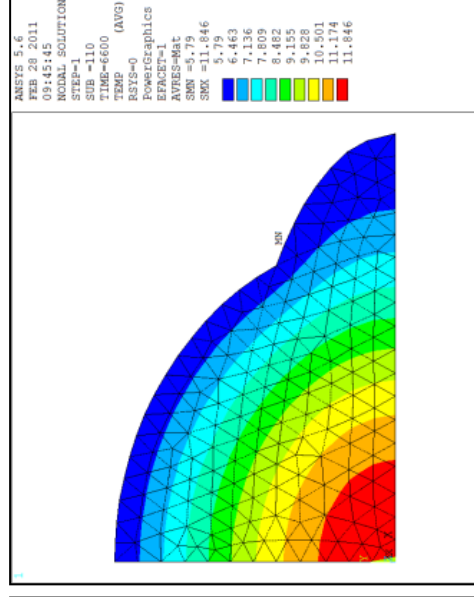
Figure 4: Using “ellipsoidal” mass-diffusivity of to predict moisture profiles in the ellipsoid oblate.



a)  $t = 180$  s

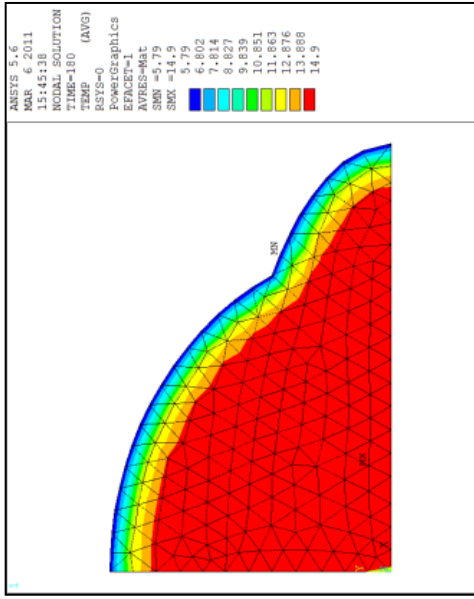


b)  $t = 900$  s

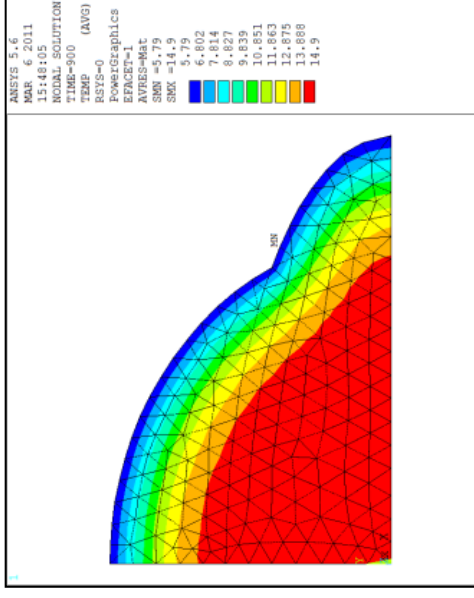


c)  $t = 6600$  s

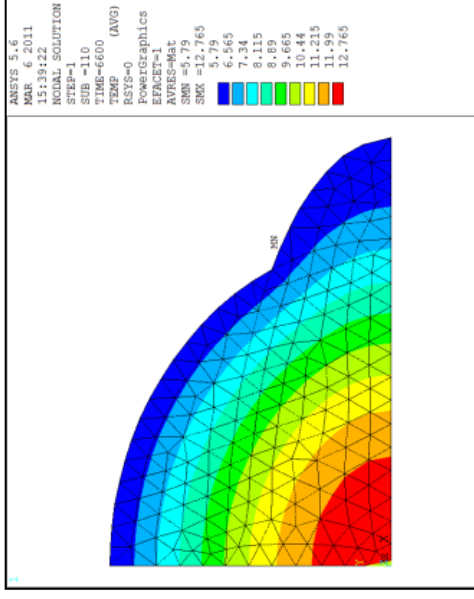
Figure 5: Using “spherical” mass-diffusivity of to predict moisture profiles in the revolution volume.



a)  $t = 180$  s

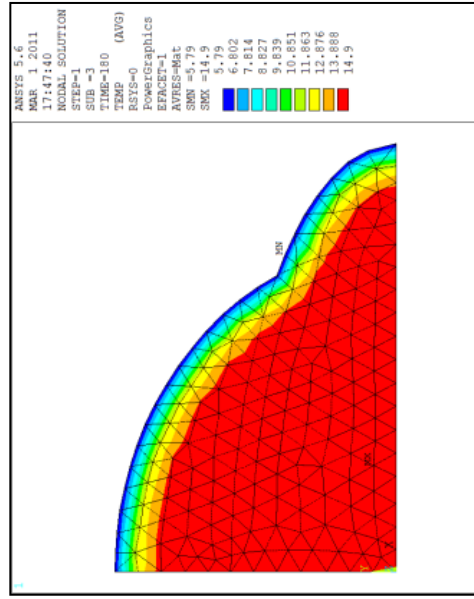


b)  $t = 900$  s

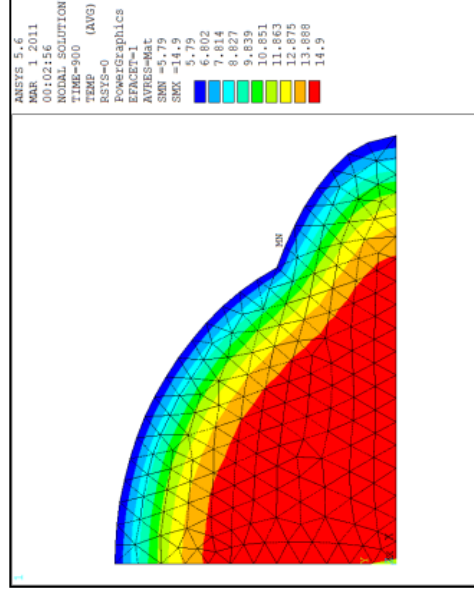


c)  $t = 6600$  s

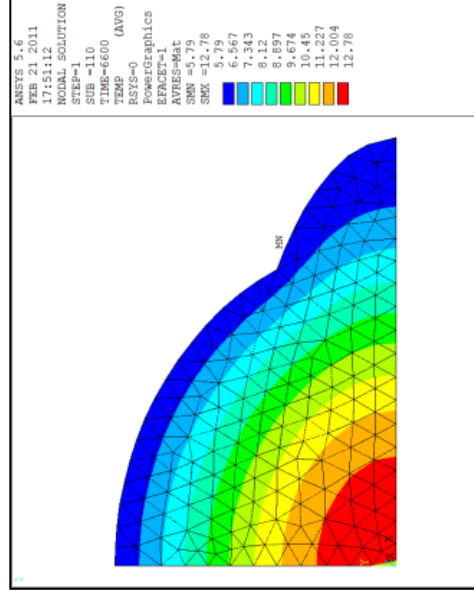
Figure 6: Using “elipsoidal” mass-diffusivity of to predict moisture profiles in the revolution volume.



a)  $t = 180$  s



b)  $t = 900$  s



c)  $t = 6600$  s

Figure 7: Using “revolution volume” mass-diffusivity of to predict moisture profiles in the revolution volume.

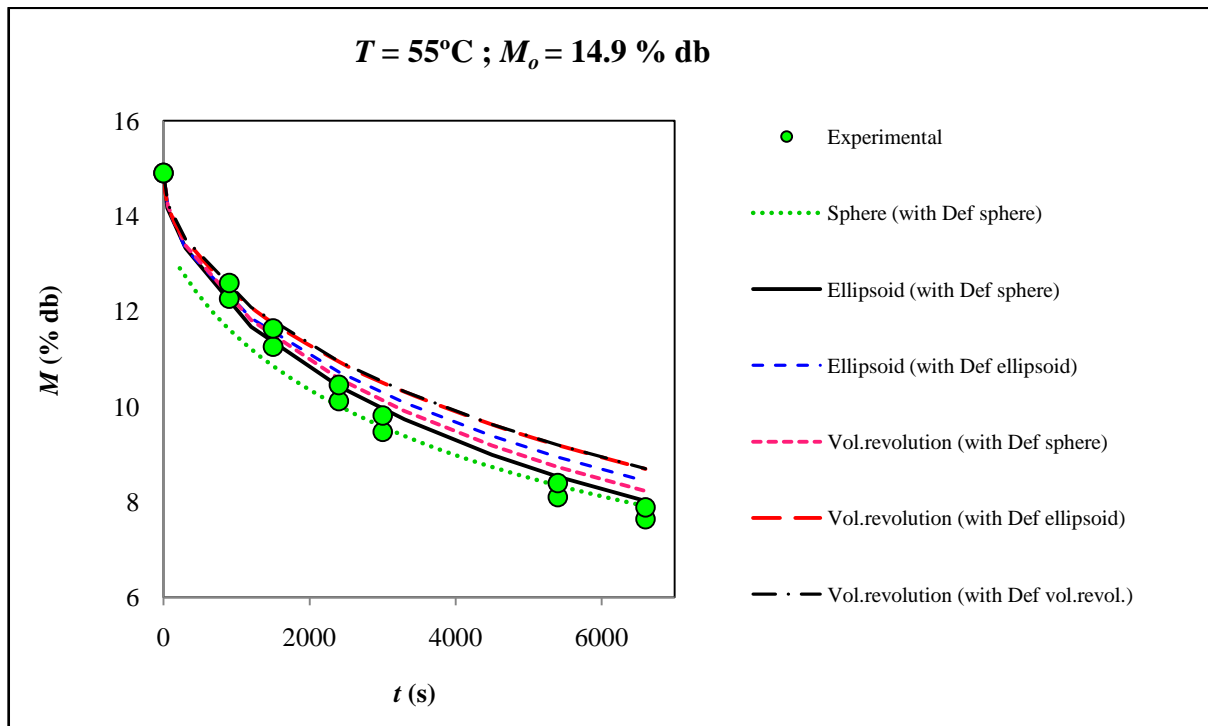


Figure 8: Experimental moisture data (points) and predicted curves by the finite elements models considering different geometries and diffusion coefficients, during the drying of amaranth grain with 14.8% db initial moisture content at 55°C.

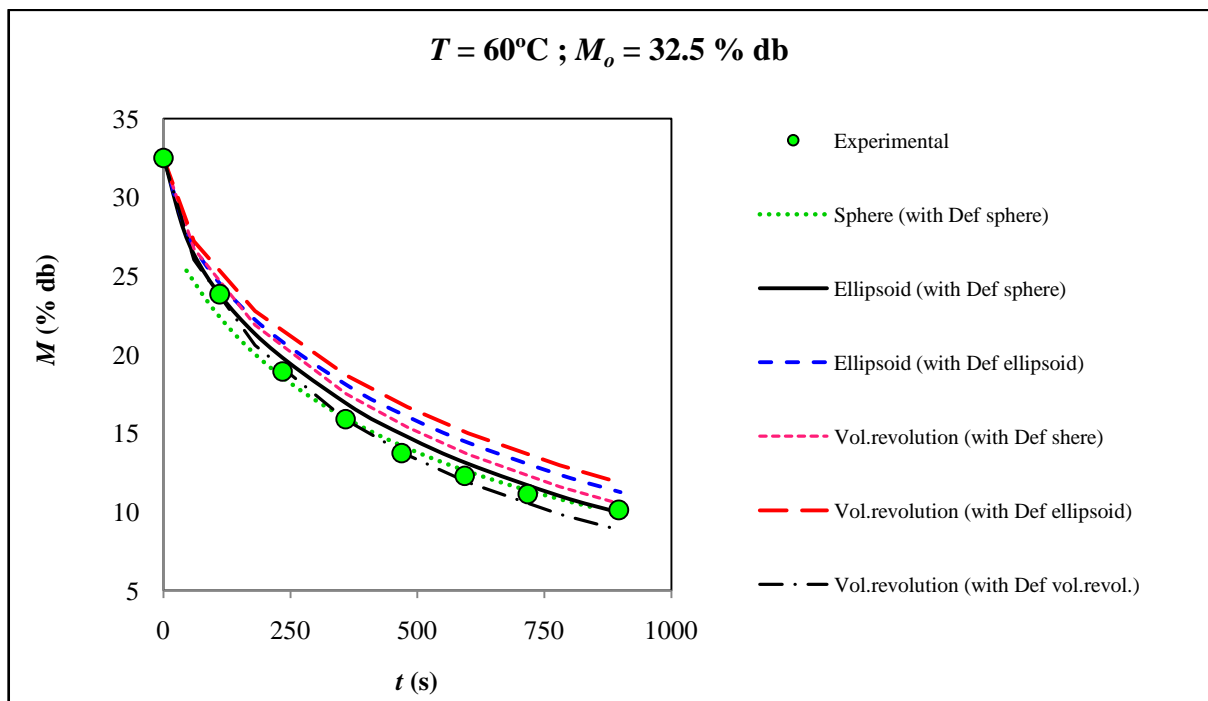


Figure 9: Experimental moisture data (points) and predicted curves by the finite elements models considering different geometries and diffusion coefficients, during the drying of amaranth grain with 32.5% db initial moisture content at 60°C.

To decide which model had the best performance, a statistical analysis based on the minimization of the sum of the squares of the residuals between measured and predicted values of moisture was made, and it was determined that the best description was obtained for ellipsoidal geometry using the diffusion coefficient of spheres.

### 3.3 Applying of the finite elements model to determine maximum $M$ , $T$ profiles

Once defined which the best of the finite element models was, the drying simulation under different conditions was made to explore and to analyze the profiles and maximum gradients of moisture and temperature into the grain during drying.

To this end, some nodes regularly spaced on the horizontal semi-axis of the ellipsoid, and also on the vertical semi-axis were selected. For these selected nodes, the evolution of the nodal humidity (nodal temperatures by analogy) during drying were simulated. As example, Figure 10a-b shows the simulated time profiles of the nodal moistures in the  $x$ -direction and in the  $y$ -direction for the experimental conditions of drying of amaranth grain with 14.9% db initial moisture at 55°C.

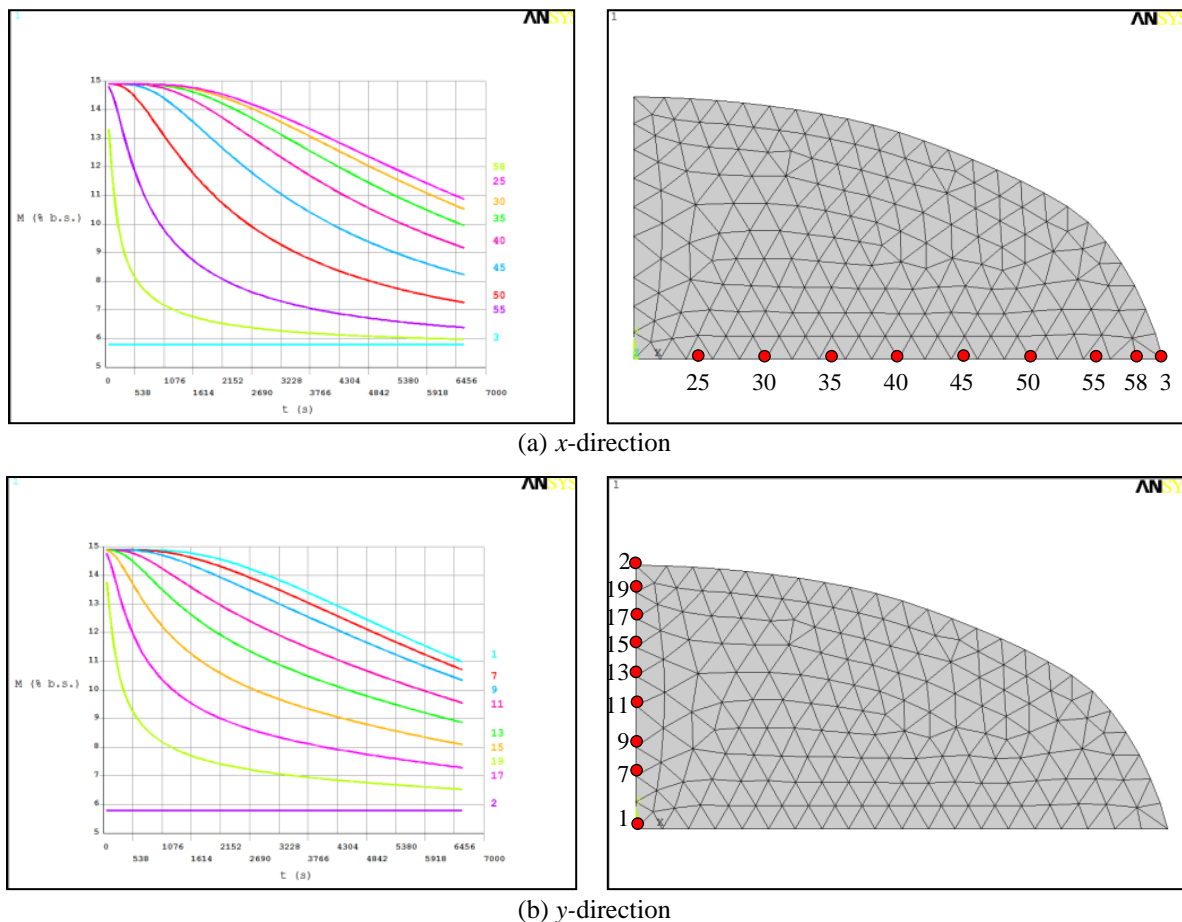


Figure 10: Simulation of moisture profiles at selected nodes located on the semi-axis horizontal ( $x$ -direction) and vertical ( $y$ -direction) of the oblate ellipsoid during drying at 55°C of amaranth grain with 14.9% db, when diffusion coefficient of spheres was used.

Since the drying process is conducted from the outside toward the center core of grain, the moisture content of the region of the core (nodes 25, 7, 1) remained almost unchanged during approximately the first 15 minutes drying time, before beginning to decline slowly over time

while nodes near the surface of the grain reached equilibrium more quickly. Profiles with similar behavior were determined by Wu et al. (2004) for drying rice grains modeled by the finite volume method, and by Haghghi and Segerlind (1988) for soybeans.

Figure 11 shows the moisture gradient along the two principal axes of grain amaranth that correspond to the length ( $x$ -direction) and width ( $y$ -direction) under the drying conditions of 55°C of temperature and 14.9% db initial moisture content. It can be seen that the moisture gradient reaches a maximum in the  $x$ -direction (i.e. in the length) of 38.3% db/mm at 20 minutes, while in the  $y$ -direction (or the width), the maximum humidity gradient takes a value of 44.49% db/mm in about 21 minutes (1260 s). This means that the maximum moisture gradient in the width direction of the grain is greater than the maximum gradient corresponding to the length ( $\max(\text{grad}M_y) / \max(\text{grad}M_x) = 1.165$ ).

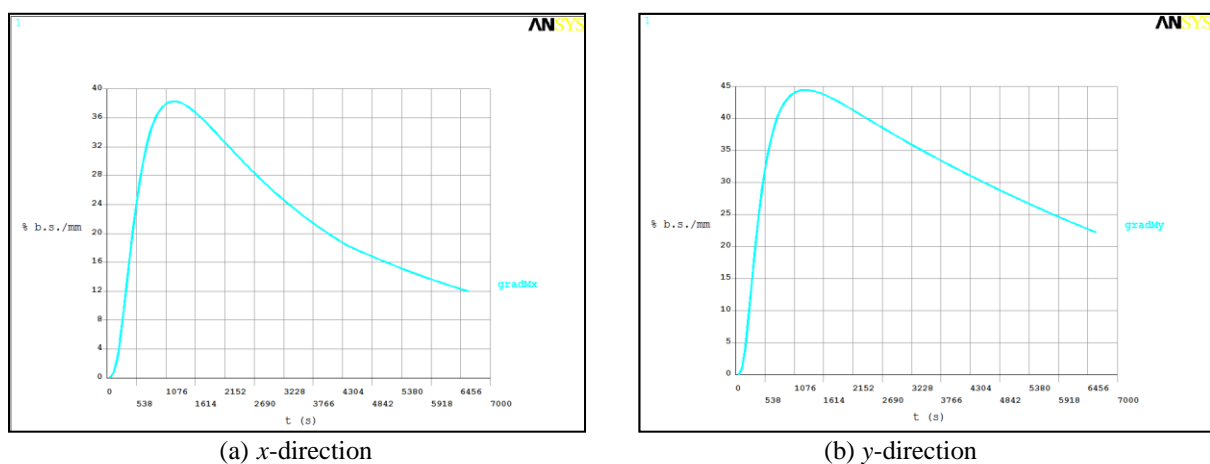


Figure 11: Gradients of moisture on the semi-axis horizontal ( $x$ -direction) and vertical ( $y$ -direction) of the oblate ellipsoid during drying at 55°C of amaranth grain with 14.9% db, when diffusion coefficient of spheres was used.

Coincidentally, Wu et al. (2004), in a study of drying rice grains described as ellipsoids by the finite volume technique, observed similar behavior in the moisture gradient, which peaks in the axial directions corresponded to the time of order 22-25 min, when drying conditions were used similar to those in this work ( $T = 60^\circ\text{C}$ ,  $M_o = 22.1\%$  db).

In a previous work, Yan et al. (2002) showed that the higher moisture gradient during drying and tempering of two-dimensional model of rice grains as an ellipse appears in the minor axis. The authors note the value of these results since moisture patterns inside the kernels are vital to understanding the formation of cracks, especially when considering the effects of glass transition.

Such studies provide useful information for determining the optimum drying and tempering of grains that result in better subsequent milling quality (Yang et al., 2002).

Figures 12 and 13 show, as example, the temperature profiles inside grain during drying at two particular drying conditions. Temperature profiles ensure the validity of the hypothesis assumed of isothermal behavior of the solid during drying, as observed since the material rapidly reaches equilibrium with the drying air temperature (in about 20 s for the conditions 60°C of drying temperature, 32.5% db initial moisture content of grain, 3 m/s of air velocity, 25°C of initial grain temperature; and in approximately 1.5 min at 55°C of drying temperature, 14.9% db initial moisture content of grain, 0.3 m/s of air velocity, 25°C of initial grain temperature). Yang et al. (2001), in a study of drying rice grains at 60°C showed that the temperature of the nodes reaches the value of the drying air temperature in just 3 minutes.

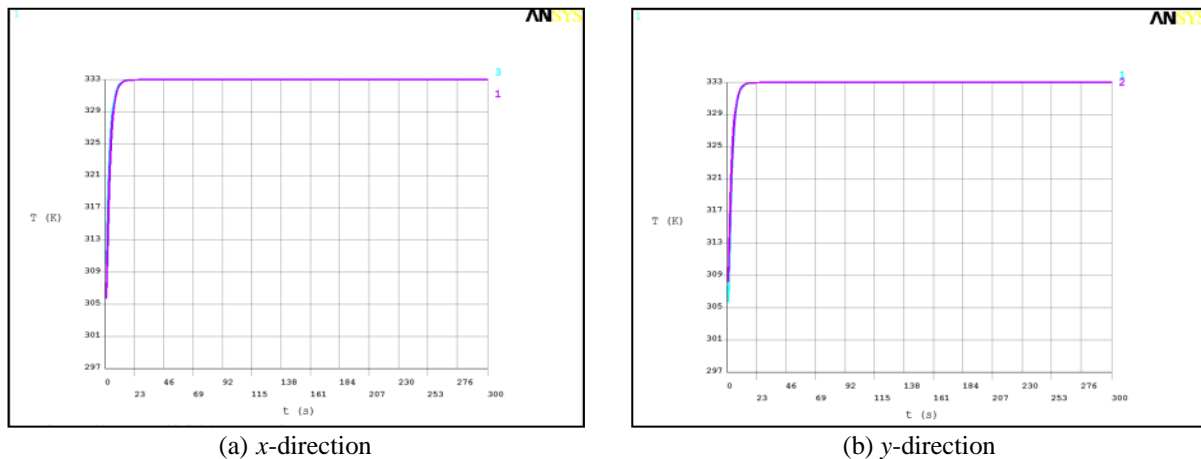


Figure 12: Profiles of nodal temperatures on the semi-axis horizontal ( $x$ -direction) and vertical ( $y$ -direction) of the oblate ellipsoid during drying of amaranth grain with 32.5% db at 60°C and 3 m/s, when diffusion coefficient of spheres was used.

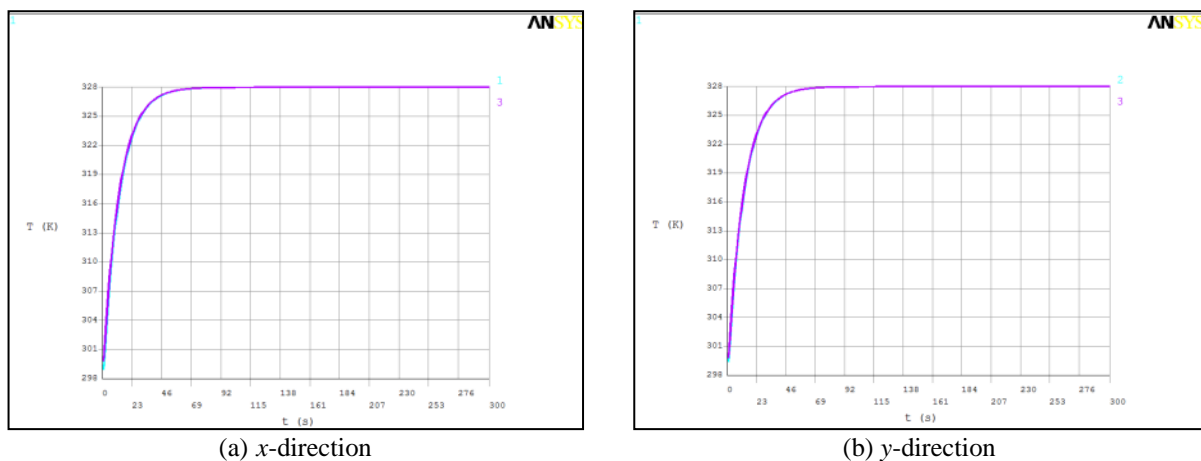


Figure 13: Profiles of nodal temperatures on the semi-axis horizontal ( $x$ -direction) and vertical ( $y$ -direction) of the oblate ellipsoid during drying of amaranth grain with 14.9% db at 55°C and 0.3 m/s, when diffusion coefficient of spheres was used.

#### 4 CONCLUSIONS

A finite element formulation implemented in ANSYS<sup>®</sup> using the direct analogy of thermal-mass diffusion could be used to obtain numerical solutions to the simultaneous equations of heat and mass diffusion that describe the removal of moisture and heat gain during the isothermal drying of amaranth grain, for temperatures from 25 to 70°C and initial moisture contents between 14.9 and 32.5% db (dry basis).

The parametrical model constructed considered two-dimensional domains attending different geometries (sphere, oblate ellipsoid, volume of revolution) to describe the grain shape, discretized by 6-node triangular elements with characteristics of axial symmetry. Grain surface instantaneously attaining equilibrium moisture content (strict internal control during the drying process) was assumed as boundary condition.

Own and published experimental drying data were used to estimate the diffusion coefficient of moisture and to validate the finite elements model by contrasting of measured values and predicted of average moisture content. Diffusivities resulted between  $1.538 \times 10^{-12}$

$\text{m}^2/\text{s}$  and  $4.334 \times 10^{-11} \text{ m}^2/\text{s}$  for oblate ellipsoid, and between  $1.850 \times 10^{-12} \text{ m}^2/\text{s}$  and  $5.189 \times 10^{-11} \text{ m}^2/\text{s}$  for spheres, being the ratio between these coefficients equivalent to the amaranth sphericity squared. An Arrhenius type exponential dependence of the diffusion coefficient with the reciprocal of the absolute temperature, and a linear function of initial moisture content of grain was probed, resulting mean activation energy of 25.1 kJ/mol.

Best description of the drying curves was obtained when the domain was modeled by ellipsoidal geometry applying moisture diffusion coefficient of spheres.

The developed finite elements model allows predict temporal and spatial profiles of moisture and temperature in amaranth grain, the time process for reach the maximum mass and thermal gradients, and ensure the validity of the hypothesis assumed isothermal behavior of the solid during drying.

## REFERENCES

- Abalone, R., Gastón, A., and Lara, M.A., Determination of mass diffusivity coefficient of sweet potato. *Drying Technology. An International Journal* 18(10):2273-2290, 2000.
- Abalone, R., Casinera, A., Gastón, A., and Lara, M.A., Comparison of thin layer equations for drying of amaranth seeds. *Trabajos del X Congreso CYTAL "Congreso Argentino de Ciencia y Tecnología de Alimentos" y 1er. Simposio Internacional de Nuevas Tecnologías*, (ISBN 987-22165-1-7), 1° Ed. AATA-FONCYT-AGENCIA Nacional de Promoción Científica y Tecnológica, Buenos Aires, 1(4):1396-1404, 2006a.
- Abalone, R., Cassinera, A., Gastón, A., and Lara, M.A., Some physical properties of amaranth seeds. *Biosystems Engineering*, 89(1):109–117, 2004.
- Abalone, R., Gastón, A., Casinera, A., and Lara, M.A., Thin layer drying of amaranth seeds. *Biosystems Engineering*, 93(2):179-188, 2006b.
- Aguerre, R.J., Gabbitto, J.F., and Chirife, J., Shape factors for the analysis of diffusion in air drying of grains. *International Journal of Food Science and Technology*, 22:701–705, 1987.
- Álvarez, C. A., Aguerre, R., Gómez, R., Vidales, S., Alzamora, S.M., and Gerschenson, L.N., Air dehydration of strawberries: effects of blanching and osmotic pretreatments on the kinetics of moisture transport. *Journal of Food Engineering*, 25:167-178, 1995.
- Bakalis, S., Kyritsi, A., Karathanos, V.T., and Yanniotis, S., Modeling of rice hydration using finite elements. *Journal of Food Engineering*, 94(3&4):321–325, 2009.
- Becker, H.A., A study of diffusion in solids of arbitrary shape with application to the drying of the wheat kernel. *Journal of Applied Polymer Science*, 1(2): 212-226, 1959.
- Becker, H.A., and Sallans, H.R. A study of internal moisture movement in the drying of the wheat kernel. *Cereal Chemistry*, 32:212-226, 1955.
- Brooker, D., Bakker-Arkema, F.W., and Hall, C.W., *The Drying and Storage of Grains and Oilseeds*, Van Nostrand Reinhold, Avi Book, New York, 1992.
- Calzetta Resio, A.N., Aguerre, R.J., and Suárez, C., Drying characteristics of amaranth grain. *Journal of Food Engineering*, 65(2):197-203, 2004.
- Choi, Y., and Okos, M.R., Effects of temperature and composition on the thermal properties of foods. *Food Engineering and Process Applications*, Elsevier Applied Science Publishers, London, 1:93-101, 1986.
- Crank, J., *The Mathematics of Diffusion*. Oxford University Press, New York, 1964.
- De Queiroz, D.M., and Couto, S.M., Simulando o processo de redistribuição de umidade no interior de um grão de arroz durante o período de repouso. Departamento de Engenharia Agrícola, Universidade Federal de Viçosa, Brasil, 2006.
- Demirel, D., and Turhan, M., Air-drying behavior of Dwarf Cavendish and Gros Michel banana slices. *Journal of Food Engineering* 59:1-11, 2003.

- Doymaz, I., and Pala, M., The thin-layer drying characteristics of corn. *Journal of Food Engineering*, 60(2):125-130, 2003.
- Doymaz, I., Drying behaviour of green beans. *Journal of Food Engineering*, 69(2):161-165, 2005.
- FAO, *CD-ROM de Cultivos Andinos, Memorias de la Reunión Técnica y Taller de Formulación de Proyecto Regional sobre Producción y Nutrición Humana en Base a Cultivos Andinos*, Editores: A. Mujica Sánchez-J. Izquierdo-J. P. Marathee-C. Morón-S.E. Jacobsen, <http://www.rlc.fao.org/es/agricultura/produ/cdrom/contenido/libro07/home7.htm>, Arequipa, Perú, 1999.
- FAO, El Cultivo del Amaranto (*Amaranthus* spp.): Producción, Mejoramiento Genético y Utilización, Oficina Regional de la FAO para América Latina y el Caribe, <http://www.rlc.fao.org/es/agricultura/produ/cdrom/contenido/libro01/home1.htm>, 1997.
- Gabitto, J., and Aguerre, R.J., Heat and mass transfer processes in bodies of non conventional shapes. *International Communication in Heat and Mass Transfer*, 13:691-700, 1986.
- Gastón A., Abalone, R.M., Giner S.A., Coeficientes de difusión en trigo como elipsoide axisimétrico y esfera. Aplicación del Método de los Elementos Finitos a datos de secado con aire. *Memorias del 8º Congreso de Transferencia de Calor y Materia*, Veracruz, México, 184-189, 2001a.
- Gastón, A.L., Abalone, R.M., and Giner, S.A., Wheat drying kinetics. Diffusivities for sphere and ellipsoid by finite elements. *Journal of Food Engineering*, 52:313-322, 2002.
- Gastón, A.L., Abalone, R.M., Giner, S.A., and Bruce, D.M., Applying the finite element method to drying kinetics data of Prointa-Isla Verde and Broom wheat cultivars represented as spheres and ellipsoids. *Proceedings of ENPROMER 2001*, Vol. III: 1651-1656, 2001b.
- Gastón, A.L., Abalone, R.M., Giner, S.A., and Bruce, D.M., Effect of modelling assumptions on the effective water diffusivity in wheat. *Biosystems Engineering*, 88(2):175-185, 2004.
- Gastón, A.L., Abalone, R.M., Giner, S.A., and Bruce, D.M., Geometry effect on water diffusivity estimation in ProInta, Isla-Verde and Broom wheat cultivars. *Latin American Applied Research*, 33:327-331, 2003.
- Giner, S.A., Mascheroni, R.H., Diffusive drying kinetics in wheat, Part 1: potential for a simplified analytical solution. *Journal of Agricultural Engineering Research*, 80(4):351-364, 2001.
- Giner, S.A., Mascheroni, R.H., PH—Postharvest Technology: diffusive drying kinetics in wheat, Part 2: applying the simplified analytical solution to experimental data. *Biosystems Engineering*, 81(1):85-97, 2002.
- Haghighi, K., and Segerlind, L.J., Modeling simultaneous heat and mass transfer in an isotropic sphere—a finite element approach. *Transactions of the ASAE*, 31(2):629-637, 1988.
- Holman, J.P., *Heat Transfer*, 4th edn. McGraw-Hill, New York, 1976.
- Ibarz-Ribas, A., and Barbosa-Cánovas, G.V., *Operaciones Unitarias en la Ingeniería de Alimentos*. Colección Tecnología de Alimentos. Ed. Mindi-Prensa, Barcelona, España, 2005.
- INTA, Instituto Nacional de Tecnología Agropecuaria - Argentina, *Redescubren las propiedades nutritivas del amaranto*, Noticias - INTA en los medios, Nota 12 de 91, 26/07/2011.
- Lema, A., Palumbo, D., Adaro, J., and Lara, M., Equilibrio de sorción para Amaranto, *Memorias del 81 Congreso de Transferencia de Calor y Materia*, pp 184-189, Veracruz, Mexico, 2001.
- López, A., Vírveda, P., and Abril, J. Influence of dry matter content and drying conditions on effective diffusion coefficient of onion (*Allium cepa*, L.). *Drying Technology*, 13(8-9): 2181-2190, 1995.

- Lu, R., and Siebenmorgen, T.J., Moisture diffusivity of long-grain rice components. *Transactions of the ASAE*, 35(6):1955-1961, 1992.
- Madamba, P.S., Driscoll, R.H., and Buckle, K.A., The thin layer drying characteristic of garlic slices. *Journal of Food Engineering*, 29:75-97, 1996.
- Madenci, E., and Guven, I., *The Finite Element Method and Applications in Engineering using Ansys®*. Springer Science+Business Media, LLC, NY 10013, USA, 2006.
- Márquez, C.A., De Michelis, A., and Giner, S.A., Drying kinetics of rose hip fruits (*Rosa eglanteria* L.). *Journal of Food Engineering*, 77(3):566-574, 2006.
- Mohapatra, D., and Rao, P., A thin layer drying model of parboiled wheat. *Journal of Food Engineering*, 66(4):513-518, 2005.
- Muthukumarappan, K., and Gunasekaran, S., Vapor diffusivity and hygroscopic expansion of corn kernels during adsorption. *Transactions of the ASAE*, 33(5):1637-1641, 1990.
- Pagano, A.M., and Mascheroni, R.H. Water sorption of *Amaranthus cruentus* L. seeds modelled by G.A.B. equation. *International Journal of Food Properties*, 6(3):329-340, 2004.
- Pagano, A.M., and Mascheroni, R.H., Sorption isotherms for amaranth grains. *Journal of Food Engineering*, 67(4):441-450, 2005.
- Pagano, A.M., and Mascheroni, R.H., Thin-layer drying of amaranth grains. *Trabajos del X Congreso CYTAL "Congreso Argentino de Ciencia y Tecnología de Alimentos" y Ier. Simposio Internacional de Nuevas Tecnologías* (ISBN 987-22165-1-7), AATA-FONCYT-AGENCIA Nacional de Promoción Científica y Tecnológica, 1º Edición, Buenos Aires, 1(4):1422-1429, 2006.
- Panchariya, P.C., Popovic, D., and Sharma, A.L. Thin-layer modeling of black tea drying process. *Journal of Food Engineering*, 52(4):349-357, 2002.
- Ronoh, E.K., Kanali, C.L., Mailutha, J.T., Shitanda, D., Thin layer drying kinetics of amaranth (*Amaranthus cruentus*) grains in a natural convection solar tent dryer. *African Journal of Food Agriculture Nutrition and Development*, 10(3):2218-2233, 2010.
- Ruiz-López, I.I, Ruiz-Espinosa, H., Luna-Guevara, M.L., and García-Alvarado, M.L., Modeling and simulation of heat and mass transfer during drying of solids with hemispherical shell geometry. *Computers and Chemical Engineering*, 35:191-199, 2011.
- Servieres, D.L., and Giner, S.A., Secadoras discontinuas de granos. Desarrollo de un modelo y programa de simulación de diseño básico. *Departamento de Ingeniería Química UNLP, Argentina*, 57 págs., 1997.
- Steffe, J.F., and Singh, R.P., Rough rice tempering. *ASAE Paper N° 79-3348*, St. Joseph, MI, 1979.
- Szöke, Sz., Wertz, V. and Persoons, E., Use of temperature front parameters to compute the drying front. *Journal of Agricultural Engineering Research*, 65(4):313-323, 1996.
- Tironi, A., Crozza, D.E., and Pagano, A.M., Cinética de secado de granos de amaranto. *Proceedings VII Congreso Argentino de Ing. Rural "CADIR 2003"*, Balcarce, Argentina, 2003.
- Tosi, E.A. and Re, E.D., Amaranth grain drying in fluidised bed, *Drying Technology*, 17(4-5):909-914, 1999.
- Tosi, E.A. and Re, E.D., Amaranto. Su aplicación en la alimentación humana, *Aposgran*, 82(2):15-16, 2003.
- Vizcarra-Mendoza, M.G., Martínez-Vera, C., and Caballero-Domínguez, F.V., Thermal and moisture diffusion properties of amaranth seeds. *Biosystems Engineering*, 86(4):441-446, 2003.
- Waezi-Zadeh, M., Ghazanfari, A., and Noorbakhsh, S., Finite element analysis and modeling of water absorption by date pits during a soaking process. *Journal of Zhejiang University-*

- Science B (Biomedicine & Biotechnology)*, 11(7):482-488, 2010.
- Weber, L.E., *Amaranth Grain Production Guide*. Rodale Research Center, Rodale Press Inc., Pennsylvania, USA, 1987.
- Wu, B., Yang, W., and Jia, C., A three-dimensional numerical simulation of transient heat and mass transfer inside a single rice kernel during the drying process. *Biosystems Engineering*, 87(2):191–200, 2004.
- Yang, W., Jia, C., Siebenmorgen, T.J., Howell, T.A., and Clossen, A.G., Intra-kernel moisture responses of rice to drying and tempering treatments by finite element simulation. *Transactions of the ASAE*, 45(4):1037–1044, 2002.
- Yang, X., Yang, W., Siebenmorgen, T. J., and Jia, C., Extending the capability of ANSYS to simulate the biomechanics of rice drying. *2001 IFT Annual Meeting*, June 23-June 27; New Orleans, LA, Paper 73C-31, [http://ift.confex.com/ift/2001/techprogram/paper\\_8866.htm](http://ift.confex.com/ift/2001/techprogram/paper_8866.htm), 2001.
- Yoon, S., and Han, B., On moisture diffusion modeling using thermal-moisture analogy. *Journal of Electronic Packaging*, 129(4):421-426, 2007.